A Novel Cell Irradiation System Using 90°-Scattering Technique

I. C. Cho, M. F. Weng, J. M. Wu, S. Y. Chiang, W. T. Chou, H. Niu, and C. H. Hsu, *Member, IEEE*

***Abstract*—A novel cell irradiation system was developed for use with the HVEE Van de Graaff accelerator at the National Tsing Hua University. A 90°-scattering technique using an Au foil was designed, in which charged particles were directed from horizontal to vertical irradiation. Beam performance was tested with a silicon detector and a CR-39 nuclear track detector. The HeLa cells were irradiated with 2-MeV alpha particles and the formation of giant cells was observed. The result showed that this system provides a convenient way of generating a vertical particle beam and a cell-supporting chamber, thereby allowing a suitable cell growth condition during irradiation. Furthermore, establishment of such a system is more convenient and economical than the alternatives.**

***Index Terms*—Accelerator, biological effect of radiation, ion beam applications.**

I. Introduction

THIS study deals with an ion beam irradiation system designed for radiobiological applications at the Accelerator Laboratory of the National Tsing Hua University, Taiwan. While setting up an irradiation system, several issues had to be taken into account, such as beam direction, flux intensity, and uniformity. With respect to beam direction, irradiating systems can be classified into horizontal and vertical designs. Some laboratories, such as the LBL (Berkeley, USA), GSI (Darmstadt, Germany), and CENBG (Bordeaux, France), chose the horizontal beam design. Others, including Columbia University (New York, USA), JAERI (Takasaki, Japan), and MIT (Boston, USA), chose the vertical beam design [1]. Both these designs are successfully applied for cell irradiation; however, in the horizontal design, the cell motion caused by gravity is an intrinsic problem for cell irradiation [2]. With regard to keeping the cell samples immobile, the vertical design is more suitable for cell irradiation than the horizontal design. Unfortunately, most beams provided by particle accelerators are horizontal. To resolve this problem, a 90° magnet is needed to bend the beam vertically. However, it demands ample space and funds. Furthermore, to avoid spreading of the beam after passing through the 90° magnet, an additional beam-reforming system is needed, and to meet the requirements of biological studies, the beam must be kept at low intensity [1].

This study used the 90°-scattering technique on the irradiating system design, in which a gold foil was used as a scattering target, instead of a 90° magnet, to scatter proton and alpha particles. This is a novel concept in vertical irradiation system designs. Moreover, this system provides low-particle intensity, which is much more suitable for radiobiological experiments.

II. Materials and Methods

A radiobiological cell irradiation station was installed at the High Voltage Engineering Europe (HVEE) 3-MV Van de Graaff accelerator at the Accelerator Laboratory of the National Tsing Hua University, Taiwan. It is capable of providing 0.8–3 MeV of proton and alpha particles with 1–20 μA of beam current. A schematic view of the irradiation system is shown in Fig. 1. The basic design of the system has an ultrathin foil to scatter the incident particles from horizontal to vertical irradiation. The Rutherford scattering formulas (1) and (2) show the scattering cross-section and the transferred kinetic energy [3], [4].

$$\sigma = \frac{1}{4}\left(\frac{Z_1 Z_2 e^2}{2E_0}\right)\csc^4\frac{\psi}{2} \tag{1}$$

$$E_1 = E_0\left(\frac{M_1}{M_1+M_2}\right)^2\left[\cos\psi + \sqrt{\left(\frac{M_2}{M_1}\right)^2 - \sin^2\psi}\right]^2 \tag{2}$$

where Z_1, Z_2 and M_1, M_2 are the atomic number and the particle mass of the incident particle and the target atom, respectively; E_0 and ψ are the incident particle energy and the scatter angle, respectively; and E_1 is the energy of the scattered particle. When the incident particle collides with the target atom and gets scattered, the energy of the scattered particle depends on the scattering angle, the incident particle energy, and the depth of the collision event. Therefore, the energy lost with depth must be taken into account when using a thick target. The new energy of the incident particle E_0' at depth x can be defined by (3). Furthermore, the energy of the scattered particle E_1' from depth x can be derived from (4), where $(dE/dx)_{in}$ and

Manuscript received April 21, 2010; revised August 03, 2010 and September 10, 2010; accepted September 27, 2010. Date of publication November 09, 2010; date of current version February 09, 2011. This work was supported by the National Science Council under Grants NSC96-2221-E-007-065-MY3 and NSC98-2221-E-007-110-MY2.

I. C. Cho, W. T. Chou, and C. H. Hsu are with the Department of Biomedical Engineering and Environmental Sciences, National Tsing Hua University, Hsinchu 30013, Taiwan.

M. F. Weng is with the National Synchrotron Radiation Research Center, Hsinchu 30076, Taiwan and also with the Department of Applied Chemistry, National Chiao Tung University, Hsinchu 30010, Taiwan.

J. M. Wu is with the Department of Radiation Oncology, E-Da Hospital, Jiau-Shu Tsuen, Yan-Chau Shiang, Kaohsiung County 824, Taiwan, and also with the Department of Medical Imagines and Radiological Science, I-Shou University, Jiau-Shu Tsuen, Yan-Chau Shiang, Kaohsiung County 824, Taiwan.

S. Y. Chiang is with the National Synchrotron Radiation Research Center, Hsinchu 30076, Taiwan.

H. Niu is with Nuclear Science and Technology Development Center, National Tsing Hua University, Hsinchu 30013, Taiwan (e-mail: hniu@mx.nthu.edu.tw).

Color versions of one or more of the figures in this paper are available online at http://ieeexplore.ieee.org.

Digital Object Identifier 10.1109/TNS.2010.2087036

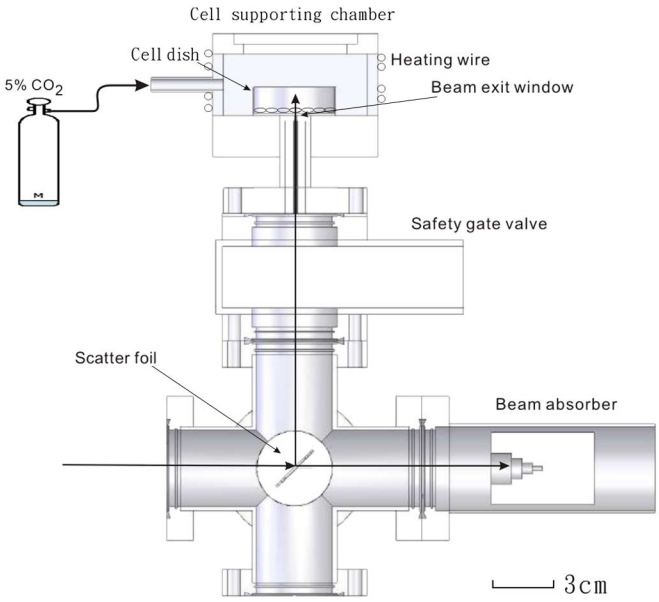

Fig. 1. A schematic view of the 90°-scattering irradiation system. The Au foil is 100 nm at a tilt angle of 45°, and the beam exit window is 1 mm in diameter.

$(dE/dx)_{out}$ are the stopping powers of the incident and the outgoing particles, respectively, in a specific material with specific energy. The scattered particle intensity at the beam exit window can be estimated by (5), where I_{in} and I_{exit} are the intensities of the incident and the exiting beams. n_t and $d\Omega$ are the atomic densities of the target material and the scattering solid angle, respectively. Based on these equations, one can arrive at some conclusions. The cross-sections in (1) decreased very quickly with the scattering angle, but in the vertical system design, the scattering angle was $\psi = 90°$. To compensate the loss of scattering efficiency, a high Z target was required in the system design. For this reason, gold was the appropriate choice to fabricate the self-supporting thin film target. Even though a thicker target could give a higher scattering efficiency, the energy range of the scattered particles was also wide, and this may complicate the ensuing absorbed dose estimation in a cell irradiation experiment. Therefore, a nearly mono-energy vertical beam was obtained by the 90°-scattering method with an ultrathin self-supporting foil. The Au foil was placed at the center of the scattering chamber and tilted to 45°.

$$E_0' = E_0 - \left(\frac{dE}{dx}\right)_{in} \Delta x \tag{3}$$

$$E_1' = E_0' \left(\frac{M_1}{M_1 + M_2}\right)^2 \left[\cos\psi + \sqrt{\left(\frac{M_2}{M_1}\right)^2 - \sin^2\psi}\right]^2 - \left(\frac{dE}{dx}\right)_{out} \frac{\Delta x}{|\cos\psi|} \tag{4}$$

$$I_{exit} = I_{in} \cdot n_t \cdot \Delta x \cdot d\Omega \tag{5}$$

Using a quartz crystal monitor, the thickness of the Au foil was measured to be 100 nm. A carbon plate with a hole of 3-mm diameter was placed in front of the foil. This acted as a beam collimator, which limited the spot size on the foil. The beam exit window was 1 mm in diameter, which was covered with a 100-nm silicon nitride membrane to seal the vacuum. The silicon nitride membrane was fabricated by the method proposed by Ciarlo, in which the silicon nitride was deposited by the LPCVD technique with 85% SiH_2Cl_2 and 17% NH_3 at 850°C [5]. In this system, only a small portion of the incident particles was scattered in an arbitrary solid angle and penetrated the beam exit window. The largest portion of the incident particles passed through the ultrathin foil and was absorbed by the carbon absorber. This carbon absorber was used to reduce the bremsstrahlung radiation caused by the energetic particle bombardment on the chamber wall.

TABLE I
THE GENERAL PARAMETERS OF THE IRRADIATION SYSTEM

Accelerator	HVEE KN accelerator
Beam type	Proton & alpha
Accelerate voltage	0.6 ~ 2.5 MV
Beam current	1~20 μA
Scatter foil	100 nm Au *
Scatter foil tilted angle	45°
Beam aperture	1 mm Ø
Window membrane	100 nm Si_3N_4
Beam flux	200~500 particles/s·μA
Cell-supporting chamber	70×70×30 mm^3, kept at 37℃, constant supply of humid air with 5% CO_2

*Au foil thickness is variable.

III. IRRADIATION SYSTEM PERFORMANCE

Irradiation performance tests included scattering efficiency, particle track detection, and energy spectrum measurement. In the scattering efficiency and energy spectrum measurement tests, the protons scattered by Au foil were measured by a silicon detector that was mounted above the beam exit window. To prevent the foil from being burned out or deformed at the high beam current, the 2-MeV proton beam current was operated at 1.5 μA. The measured spectrum is shown in Fig. 2, where the mean energy of the scattered protons is 1.97 MeV with an FWHM of 30 keV. Using 100 nm of Au foil gives a mean proton fluence rate of about 285 $\mathrm{particles/mm^2/s}$ at 1-μA beam current. However, using 150 nm of Au foil gives a mean proton flux of about 545 $\mathrm{particles/mm^2/s}$ at 1-μA beam current (data not shown).

In the beam uniformity test, a CR-39 film was placed above the beam aperture to trace the distribution of the scattered protons. The CR-39 track detector is commonly used for charged particle track detection [6], [7]. When the charged particles bombard into CR-39, they deposit energy and cause defects inside the detector. These defects can be developed by an etching solution and observed by a microscope. After irradiation, CR-39 was developed by 7.25N NaOH at 60°C for 1.5 h. Fig. 3 shows the phase contrast image of the CR-39 etching result, which indicates that the distribution of the etching spots is very uniform and that the cell within the irradiation region

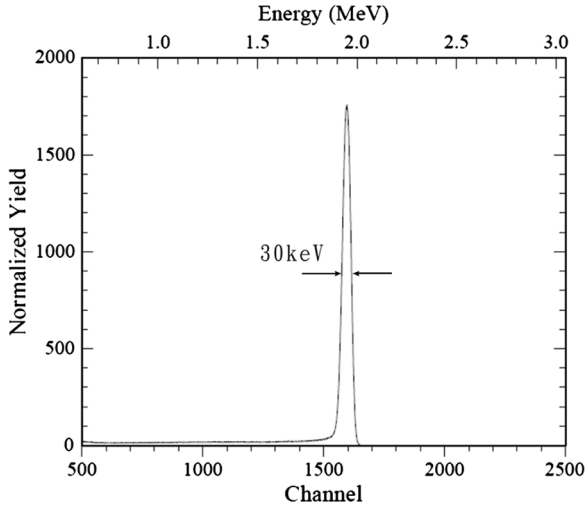

Fig. 2. The energy spectrum of scattered protons, which passed through the Si_3N_4 window and 3 mm of air gap, and then detected by the Si detector. The average energy of the scattered proton is 1.97 MeV with an FWHM of 30 keV.

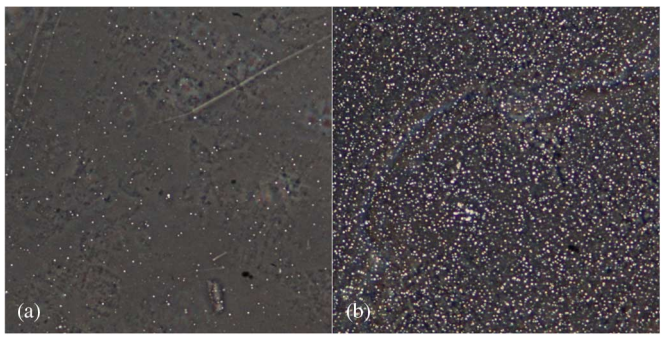

Fig. 3. The CR-39 track detection result of proton irradiation. The particle distribution of (a) a 30-s proton irradiation, (b) a 600-s proton irradiation.

will be irradiated evenly. Therefore, the authors believe that each cell was irradiated with the same intensity of particles.

The results of the energy spectrum measurement pointed out some advantages of the irradiation system. First, the FWHM of the scattered proton energy was only 1.5%. It was sufficiently low and in agreement with the Monte Carlo simulation result [8]. The energy spread was insignificant and can be neglected in the cell-absorbed dose calculation. Second, the ratio of the scattered particles to the incident particles can be easily adjusted by changing the thickness of the Au foil. The measured scattering ratio of the 150-nm Au foil was about twice (1.91) that of the 100-nm Au foil. Furthermore, the ratio can be increased to a large extent as the distance decreased between the exit window and the Au foil. The high beam throughput enables the irradiation system to shrink the beam aperture further. Furthermore, the cell irradiation experiment could be performed from a low-to a high-dose region by combing with a fast beam shutter, which adjusts the cell irradiation time. In the particle track detection experiment, the shape and the region of the beam aperture can be easily distinguished. In addition, the distribution of the etching spots was very uniform, indicating that the cells, which are located in the irradiation region, could be evenly irradiated and that each cell was irradiated with the same intensity of protons. According to the results mentioned earlier, the number of charged particles that irradiate the target cells can be estimated by calculating the superficial density of the cells. The cell-absorbed dose can be derived theoretically by the LET theory [9].

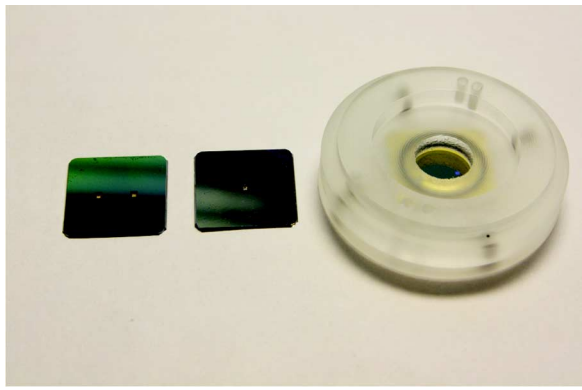

Fig. 4. The Si_3N_4 membrane and the laboratory-made cell culture dish. All the membranes were 100-nm thick. Left, the membrane was opened with two windows for the purpose of distinguishing the cells. Middle, the membrane was opened with one window for the vacuum-sealed membranes. Right, the laboratory-made cell culture dish with a slice of Si_3N_4 clipped at the bottom of the dish.

IV. Irradiation Study

The cells used for the irradiation study belonged to the HeLa cell line. The cells were cultivated in DMEM (Invitrogen) culture medium supplemented with 10% fetal bovine serum and 1% penicillin streptomycin mixture [10]. An assembled-type cell culture dish was designed for conducting cell irradiation experiments. For microscopic monitoring, the bottom of the cell dish should be thin and transparent. A photograph of the cell dish is shown in Fig. 4. The dish is composed of three plastic parts: the cover, the body, and the open-holed bottom. A 100-nm thick Si_3N_4 membrane was used as the base of the cell dish, which was placed between the body and the bottom part and clipped by an o-ring. Each membrane had two open windows, which classified the cells into an irradiation group and a control group. Before cell cultivation, the laboratory-made cell dishes were cleaned with distilled water and sterilized by ultraviolet irradiation for 24 h. The cells were planted on a Si_3N_4 membrane with a density of 100–200 $\mathrm{cells/mm^2}$ and cultivated for another 24 h. The transparent Si_3N_4 dish was found to be perfectly suitable for cell observation, and it was thin enough to minimize particle energy loss during penetration. Moreover, the cells could easily attach to the Si_3N_4 membrane and proliferate on it. Afterward, the cell dish was moved to a cell-supporting chamber and aligned with the beam aperture by an indicative light. The chamber for cell support was developed and installed above the exit window to ensure that every cell type shows a stress-free condition and maintains cell growth behavior during the irradiation procedure. The temperature and the humidity inside the cell-supporting chamber were kept at 37°C and 95%, respectively. Furthermore, the pH value of the culture medium in the chamber was kept constant by continuously flowing 5% CO_2 gas [11]. The cell-supporting system check was performed by incubating a dish of HeLa cells in the supporting chamber for 24 h. The results showed that the cell-supporting chamber can provide a stress-free condition for cell cultivation. The cells can

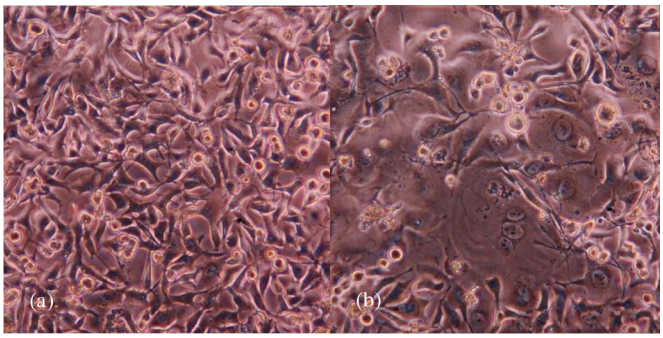

Fig. 5. The cell observation result 48 h after irradiation. The giant cell formation can be easily observed in the Irradiated group. (a) Control group, the HeLa cells planted on the unirradiated side window of laboratory-made culture dish (b) Irradiated group, the group of HeLa cells planted on the irradiate side window of the same dish.

be cultivated in the supporting chamber and observed for long durations of time. The cell dish was located at the bottom of the chamber to minimize energy loss between the exit window and the target cell, so the distance between them was kept as short as possible.

To optimize the biological response of cell irradiation in this experiment, the energy and the type of particle must be considered to allow the Bragg peak to be confined in the cell volume. According to SRIM simulation results [12], 2.0 MeV of alpha particles was chosen as the incident particles and the scattered energy was calculated to be in the range of 1.735–1.918 MeV. After penetrating two layers of the Si_3N_4 membrane—the beam exit window and the base of culture dish—the alpha particle energy corresponded to a depth from 4.8 to 5.9 μm in the culture medium, and was almost the same as the thickness of a cell nucleus. Therefore, one can predict that the Bragg peak will fall inside the cell nucleus and deliver most of the radiation energy. The possibility of double-strand break, serious cell damage, and cell death will proportionally increase with the energy imparted to the cell. Eight dishes of HeLa cell were prepared for alpha beam irradiation with eight different doses. The absorbed dose was in the range of 12–240 Gy. The cells were continuously monitored the following week after irradiation. Fig. 5 compares cells with and without irradiation. In morphology observation, the giant cells were formed in all cases 2–3 days after alpha beam irradiation. The giant cell formation indicated cell death by mitotic catastrophe, which was caused by the ion beam irradiation. Conversely, the control groups did not show any change in the cell's ability to proliferate. This observation agrees with the result of Sasaki [13].

V. Conclusion

This study established a cell irradiation system by the 90°-scattering technique, which provided suitable conditions and environment for cell irradiation. This novel system made uniform vertical irradiation feasible for radiobiological studies. Moreover, this technique can be improved and applied to the microbeam irradiation system for single-cell exposures.

References

[1] S. Gerardi, "A comparative review of charged particle microbeam facilities," *Radiat. Protect. Dosim.*, vol. 122, no. 1–4, pp. 285–291, Dec. 2006.

[2] M. Oikawa, T. Satoh, and T. Sakai *et al.*, "Focusing high-energy heavy ion microbeam system at the JAEA AVF cyclotron," *Nucl. Instrum. Methods Phys. Res. B*, vol. B260, no. 1, pp. 85–90, 2007.

[3] H. Goldstein, C. P. Poole, and J. L. Safko, *Classical Mechanics*, 3rd ed. San Francisco, CA: Addison-Wesley, 2002.

[4] J. B. Marion and S. T. Thornton, *Classical Dynamics of Particles and Systems*, 4th ed. Fort Worth, TX: Saunders College Pub., 1995.

[5] D. R. Ciarlo, "Silicon nitride thin windows for biomedical microdevices," *Biomed. Microdev.*, vol. 4, no. 1, pp. 63–68, 2002.

[6] B. Dorschel, D. Hermsdorf, and K. Kadner *et al.*, "Track parameters and etch rates in alpha-irradiated CR-39 detectors used for dosimeter response calculation," *Radiat. Protect. Dosim.*, vol. 78, no. 3, pp. 205–212, Aug. 1, 1998.

[7] D. Nikezic and K. N. Yu, "Formation and growth of tracks in nuclear track materials," *Mater. Sci. Eng.*, vol. 46, no. 3–5, pp. 51–123, 2004.

[8] L. R. Doolittle, "Algorithms for the rapid simulation of Rutherford backscattering spectra," *Nucl. Instrum. Methods Phys. Res. B*, vol. B9, no. 3, pp. 344–351, 1985.

[9] A. C. Wera, K. Donato, and C. Michiels *et al.*, "Preliminary results of proton beam characterization for a facility of broad beam in vitro cell irradiation," *Nucl. Instrum. Methods Phys. Res. B*, vol. B266, no. 10, pp. 2122–2124, 2008.

[10] M.-F. Weng, S.-Y. Chiang, and N.-S. Wang *et al.*, "Fluorescent nanodiamonds for specifically targeted bioimaging: Application to the interaction of transferrin with transferring receptor," *Diamond Rel. Mater.*, vol. 18, no. 2–3, pp. 587–591, 2009.

[11] H. Imaseki, T. Ishikawa, and H. Iso *et al.*, "Progress report of the single particle irradiation system to cell (SPICE)," *Nucl. Instrum. Methods Phys. Res. B*, vol. B260, no. 1, pp. 81–84, 2007.

[12] J. F. Ziegler, SRIM-2010, The Stopping and Range of Ions in Matter, 2010.

[13] H. Sasaki, "Lethal sectoring, genomic instability, and delayed division delay in HeLa S3 cells surviving alpha- or X-irradiation," *J. Radiat. Res.*, vol. 45, no. 4, pp. 497–508, 2004.